Cryostratigraphy of near-surface permafrost in University Valley, McMurdo Dry Valleys of Antarctica

Caitlin M. Lapalme[1], Denis Lacelle[1], Alfonso F. Davila[2], Wayne Pollard[3], Daniel Fortier[4] & Christopher P. McKay[5]
[1]*Department of Geography, University of Ottawa, Ottawa, ON, Canada*
[2]*Carl Sagan Center at the SETI Institute, Mountain View, CA, USA*
[3]*Department of Geography, McGill University, Montreal, QC, Canada*
[4]*Department of Geography, Université de Montréal, Montreal, QC, Canada*
[5]*NASA Ames Research Center, Moffett Field, CA, USA*

ABSTRACT
The presence and origin of ground ice in cold and hyper-arid regions defies the conventional understanding of ground ice forming processes. This study investigates the amount, distribution and origin of ground ice in a sand-wedge polygon in University Valley, McMurdo Dry Valleys of Antarctica. Analysis of computed tomodensitometric scans revealed three types of cryostructures: structureless, suspended, and crustal. Excess ice distribution in two permafrost cores revealed greater ice content in the center of the polygon. Water isotope analysis suggests that the ground ice was emplaced by vapour deposition, similar to two nearby polygons. The higher ground ice content in the center of the polygon is likely related to the stability of the ground surface, with a less stable surface near the shoulder of the polygon as sediments fall into cracks. The results presented in this study enhance our understanding of ground ice and the processes, including environmental factors, which form the ice-cemented permafrost in cold arid regions.

RÉSUMÉ
La présence et l'origine de la glace de sol dans les régions froides et hyperarides défie la compréhension de la formation de la glace de sol. Cette étude examine la quantité, la distribution et l'origine de la glace de sol dans un polygone situé dans la vallée de l'Université, vallées sèches de McMurdo en Antarctique. Une analyse tomodensitométrique a identifié trois types de cryostructures: sans structure, suspendue et crustale. De la glace en excès a été observée dans les deux sites d'échantillonnage, bien que la teneur en glace fût plus élevée dans le centre du polygone. L'analyse des isotopes de l'eau suggère que la glace de sol est mise en place par diffusion de vapeur et sa déposition est semblable à deux polygones situés à proximité. La teneur en glace plus élevée dans le centre du polygone est liée à la stabilité de la surface du sol, avec une surface peu stable à proximité de l'épaulement du polygone. Les résultats présentés dans cette étude améliorent notre compréhension des processus, y compris les facteurs environnementaux qui forment le pergélisol de glace cimenté dans les régions froides et sèches.

1 INTRODUCTION

Ground ice is one of the most important and dynamic geologic components of permafrost. However, its presence in the cold and hyper-arid environments of the McMurdo Dry Valleys (MDV) of Antarctica, where liquid water is rare, defies the conventional understanding of ground ice forming processes (e.g. Mackay, 1972). According to the permafrost classification map of the MDV (Bockheim et al., 2007), ground ice in permafrost occurs as: i) dry permafrost, characterized by low ice contents, usually <3% wt; ii) ice-cemented permafrost, where ice occupies the pore space of sediments; and iii) ground ice or buried ice. This broad classification mixes the abundance and genesis of ground ice, and highlights a lack of studies on the amount, distribution and origin of ground ice in this region (e.g. Marchant et al., 2002; Dickenson and Rosen, 2003; Hagedorn et al., 2010; Pollard et al., 2012; Lacelle et al., 2013). As such, the amount, distribution, and origin of ground ice in MDV permafrost remains poorly understood, yet are essential components of the dynamic relations between climate and landscape evolution.

This study investigates the cryostratigraphy of the near-surface permafrost in University Valley, a small glacial valley in the Quartermain Mountains of the MDV of Antarctica (Figure 1). Cryostratigraphy is an approach that emphasizes the description of cryostructures (distribution and shape of ground ice), the quantification of ground ice content and associated cryofacies, and the identification of discontinuities revealed by a change in cryostructure and cryofacies within permafrost. When supplemented with analyses of isotope geochemistry of the ground ice, cryostratigraphy is a powerful tool to reconstruct the history of permafrost and ground ice origin (e.g., French, 1998; French and Shur, 2010). The objective of this study is to describe the cryostructures and ground ice content in two shallow permafrost cores from University Valley by combining laboratory measurements with computed tomodensitometric scans (CT scans) that produce high-resolution images (sub-mm scale). Relations between sediment properties, cryostructures and ice content are explored. This study provides the first description of cryostructures and cryofacies in the permafrost of the MDV of Antarctica and the origin of ground ice at the study site is interpreted from δD-δ^{18}O analysis. Overall, the results presented in this study represent an additional

step towards enhancing our understanding of the processes, including environmental factors that form the ice-cemented permafrost in the Quartermain Mountains.

2 STUDY AREA

University Valley (77°52'S; 163°45'E; 1600-1800 m a.s.l.) is a 1.5 km long and 500 m wide northwest facing upper hanging glacial valley located within the Quartermain Mountains (Figure 1). A small glacier (informally named University Glacier), with a maximum thickness of ca. 150 m, is situated at the head of the valley and permanent snow patches are found scattered along the western portion of the valley floor. The local geology of the region consists of Ferrar Dolerite (Jurassic age intrusives) and sedimentary rocks of the Beacon Supergroup (Devonian to Triassic age sandstones and conglomerates) (Elliot and Fleming, 2004). Surficial sediments consist of colluvium and talus cones at the base of the valley walls and of undifferentiated till and alpine drift on the valley floor (Cox et al., 2012). Polygonal terrain developed on the valley floor and on some of the talus cones.

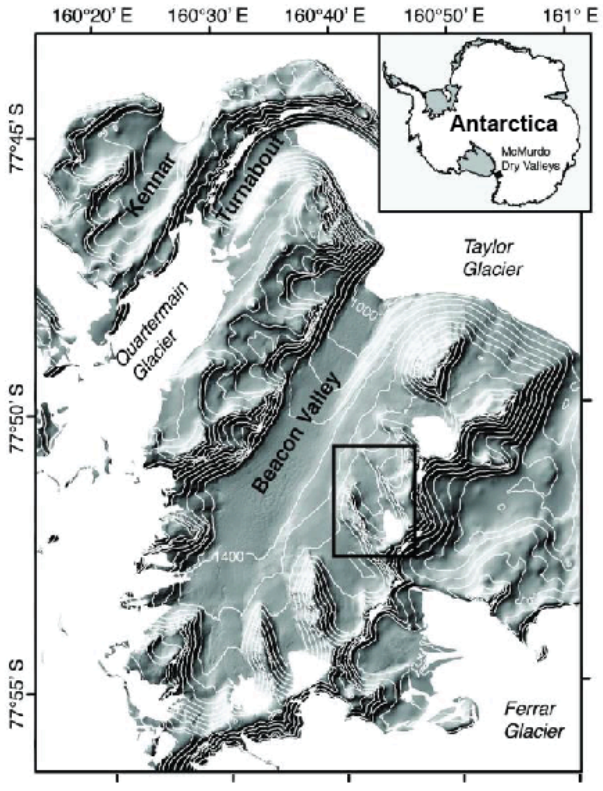

Figure 1. Map showing the location of University Valley in the Quartermain Mountains of the McMurdo Dry Valleys of Antarctica (black rectangle).

The region is located within the stable upland zone of the MDV, which is characterized by summer air temperatures <0°C and relative humidity values <50% (Marchant and Head, 2007). Mean annual air temperature recorded over a three year period from University Valley (2010-12) was -23.4 ± 0.8°C with a mean annual relative humidity of 48%. Summer air temperatures were always <0°C (maximum daily and hourly air temperature values were –5.7 and –2.8°C, respectively) for the three years; however, ground surface temperatures in central and lower University Valley rose above 0°C for a few hours on clear summer days due to solar heating (Lacelle et al., 2015).

The cold and dry climate conditions in the Quartermain Mountains ensure that the soil overlying the ice-bearing permafrost is dry and the transition between the two is termed the ice table. In University Valley, the depth of the ice table varies from 0 cm at the foot of University Glacier to more than 70 cm near the mouth of the valley (McKay, 2009; Marinova et al., 2013). It has been suggested that the depth of the ice table is controlled by snow recurrence (McKay, 2009), with a more persistent snow cover near the head of the valley. According to Mellon et al. (2013), the ice table has been at its current position for more than 10,000 years, the timescale for polygon development.

3 METHODOLOGIES

3.1 Field sampling

In January 2013, 15 shallow ice-bearing permafrost cores were collected from nine sand-wedge polygons in University Valley. This study presents preliminary results from one of these polygons (P8: 77.866°S; 160.726°E; 6 m x 15 m) where cores were obtained from the center (P8-C3, 70 cm depth) and left shoulder (P8-C6, 40 cm depth) of the polygon. This site is situated in upper University Valley and the ice table depth was 2 cm at both coring locations. The polygon was located at the fringe of the perennially cryotic zone (Lacelle et al., 2015) and according to Lacelle et al. (2013), ground ice in the uppermost 50-60 cm of two polygons situated 155 m to the southeast formed by vapour deposition.

The permafrost cores were collected using an 11.5 cm diameter Cold Regions Research and Engineering Laboratory (CRREL) core barrel equipped with a gas powerhead. Each core was retrieved in 10 to 50 cm long segments, wrapped in plastic core sleeves and shipped frozen in thermally insulated boxes to the CryoLab for Arctic, Antarctic and Planetary Studies (University of Ottawa, Ottawa, Canada) where they were kept frozen at -20°C until analysis. CT scans were first performed on the frozen cores to describe the cryostructures and extract volumetric ice content from image analysis. The permafrost cores were subsequently cut into ca. 2 cm thick slices using a RIGID circular rock saw with a 0.8 mm thick diamond blade to determine sediment properties and water content.

3.2 Cryostructures and volumetric ground ice content using CT scanning

X-ray CT scanning (computed tomodensitometric imaging) is a non-destructive method that has been employed in Arctic permafrost studies over the last decade (e.g. Calmels and Allard, 2004; Calmels and Allard, 2008; Calmels et al., 2008). The principles of CT scanning are similar to those of radiography as the process results in the 3D imaging of density contrasts in a sample. For CT scanning, density measurements are made in comparison to water and expressed in Hounsfield Units (HU) (Calmels and Allard, 2004; Calmels et al., 2010): water thus has a value of 0 HU, ice has values between ca. -250 and 750 HU, air has values near -1000 HU and sediments have values >750 HU with the actual value depending on the mineralogy of the sediment. Given the large density difference between ice, sediments and gases, the CT scanning of ice-bearing permafrost cores allows the identification of the distribution and shape of these components, and hence the identification of cryostructures. Further processing of the CT scans with image analysis software allows the estimation of volumetric ice content (Calmels et al., 2010).

The CT scanning of the full P8-C6 core and a section of the P8-C3 core was performed using a medical scanner (Siemens Somaton Volume Access) at the Institut National de la Recherche Scientifique (Québec, Canada). The permafrost cores were placed on a bench in the center of a ring that contains the X-Ray source. The X-ray source rotated around the core as the core moved down the ring resulting in an image produced through a helical movement. The scanned image stacks, with a pixel resolution of 0.4 mm, were saved in DICOM file format and analyzed using Fiji image analysis software (http://fiji.sc/Fiji) (e.g. Calmels and Allard, 2004). The images were first displayed in greyscale, where darker tones indicate lower density material (i.e., gas and ice) and lighter tones represent higher density material (i.e., sediments). The images were then processed to classify the ice component in the cores in order to explore its distribution and shape and estimate its content. Considering that the ice classification from image processing and analysis is dependent on the threshold used, four ice thresholds were tested after analyzing the peaks in the image stacks' histograms: -200 to 700 HU, -200 to 750 HU, -250 to 700 HU and -250 to 750 HU. The four thresholds yielded similar ice contents ranging within 3% for various parameters (Table 1). Therefore, the threshold with the highest ice content (-250 to 750 HU) was used to convert the CT-scanned greyscale image stack into binary images showing only the ice fraction (black represents ice; white represents all other components). These binary images were used to describe the cryostructures in the permafrost cores using the classification of Murton and French (1994): structureless, suspended, layered, lenticular, reticulate and crustal. The stack of binary images was then used to extract the volumetric ice content (CT-VIC) from each slice using the *Plot Z-axis Profile* function (0.4 mm).

Table 1: Descriptive statistics of volumetric ice content in P8-C3 and P8-C6 permafrost cores using CT-scanned images and Fiji image analysis software.

Threshold	Mean	Median	Range	Min	Max
P8-C3					
-200 to 700	27.72	20.49	68.82	3.16	71.97
-200 to 750	29.94	23.96	67.71	4.41	72.12
-250 to 700	28.85	21.26	69.06	2.85	71.91
-250 to 750	30.42	23.92	68.99	4.24	73.23
P8-C6					
-200 to 700	1.69	1.06	5.92	0.29	6.21
-200 to 750	2.14	1.44	6.53	0.65	7.18
-250 to 700	1.65	1.06	5.86	0.41	6.27
-250 to 750	2.09	1.27	6.85	0.49	7.34

3.3 Ground ice content measurements

Ice content in the permafrost cores was determined using laboratory measurements from the ca. 2 cm thick slices. The frozen slices were allowed to melt in sealed plastic bags and then transferred into graduated 50 ml polypropylene tubes. Once in the tubes, the excess ice (defined as volume of ice in the ground that exceeds the total pore volume that the ground would have under natural unfrozen conditions; van Everdingen, 1988) was determined using the equation in Kokelj and Burn (2003). The supernatant water in each sample, if present, was extracted for geochemical and isotopic analysis. The volumetric and gravimetric water contents were subsequently determined using the equation in French (2007) and using a measured sediment porosity of 0.42 ± 0.09 (Lacelle et al., 2013). The excess ice and volumetric ice content measurements were within 1 ml precision, which translate into ±1% error in the reported values. The volumetric ice content (VIC) was used to define the type of cryofacies present in the cores using the classification of Murton and French (1994): ice-poor sediments (≤25% VIC), ice-rich sediments (>25 to ≤50% VIC), sediment-rich ice (>50 to ≤75% VIC), sediment-poor ice (>75% VIC) and pure ice (100% VIC).

3.4 Water isotope analysis

The $^{18}O/^{16}O$ and D/H ratios of water samples were determined using a Los Gatos liquid water isotope analyzer. Unlike an isotope ratio mass spectrometer that measures ^{18}O and D via CO_2 and H_2 equilibration technique, respectively, this instrument directly measures the concentration of ^{18}O and D in the sample and the measurements are not affected by the salinity of the waters for total dissolved solids <10 g L-1 (Hendry et al., 2011). The results are presented using the d-notation ($\delta^{18}O$ and δD), where δ represents the parts per thousand differences for $^{18}O/^{16}O$ or D/H in a sample with respect to Vienna Standard Mean Ocean Water (VSMOW). Analytical reproducibility for $\delta^{18}O$ and δD is ±0.3‰ and ±1‰, respectively.

3.5 Grain size analysis

Grain size distribution was determined at ca. 10 cm depth intervals using the stacked sieve method. For each

analysis, ca. 30 g to 150 g of sediment was passed through seven stainless steel sieves (2 mm, 1 mm, 500 µm, 250 µm, 125 µm, 63 µm and < 63 µm). Each sample was classified into three texture classes: gravel (≥2 mm), sand (<2 mm to ≥63 µm) and fine sediments (≤63 µm). The dominant grain size was determined using the Wentworth grain size classification. Errors in the calculation of the grain size distribution for the samples arose through the occasional retention of a minimal amount of the sample in the sieve mesh and through scale measurement errors. This translates into a ±4% error in the reported values for the total particle size distribution for the samples.

4 RESULTS

4.1 Cryostructures

Based on the stack of binary images of the CT-scans, the P8-C3 core (0 to 45 cm segment) contained three types of cryostructures: structureless, suspended, and crustal.

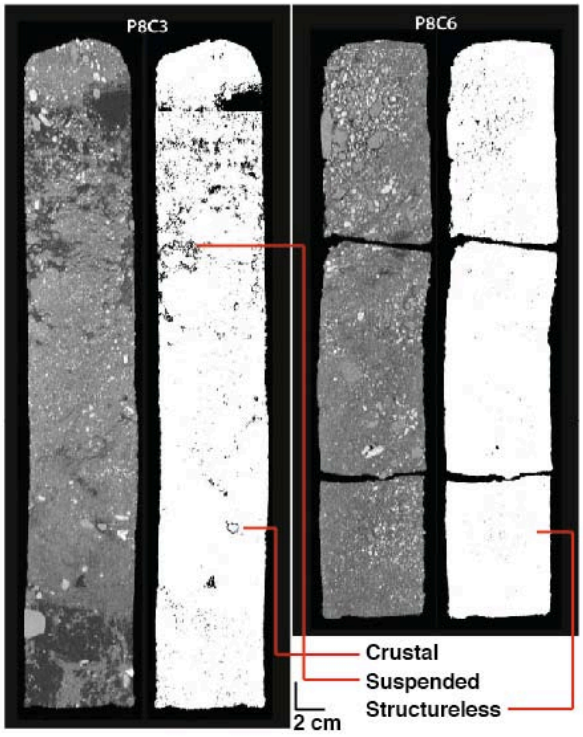

Figure 2: CT-scan images (greyscale) and processed images (black and white) for one slice along the longitudinal axis in P8-C3 (0-45 cm segment) and P8-C6 (0-40 cm) illustrating the distribution of ice, sediments and cryostructures described within the cores using the -250 to 750 HU threshold for ice.

Suspended cryostructures were observed in the near-surface (ca. 5 to 20 cm) and at multiple depths in the lower sections of the core (ca. 23 cm, 24 cm, 28 cm, 29 cm and 38 cm depths). Structureless cryostructures were present throughout the core. Crustal cryostructures were identified throughout the core (aside from 28 cm, 34 cm and 43 cm depth) as mm-thick ice coatings on individual pebbles (Figure 2; Figure 3A).

Comparatively, P8-C6 (0 to 40 cm segment) showed evidence of structureless and crustal cyrostructures only. Structureless crysotructures were observed throughout the core whereas crustal cryostructures were only observed at specific depths (e.g. 4 to 13 cm, 15 cm, 22 cm and 34 cm) (Figure 2; Figure 3B). The lenticular, layered, and reticulate cryostructures were not observed in the cores.

4.2 Ground ice content

The excess ice content and VIC in the center of the polygon (P8-C3) were much higher than the values from the left shoulder (P8-C6). Excess ice content for core P8-C3 (Figure 4A) showed two distinct bulges with depth.

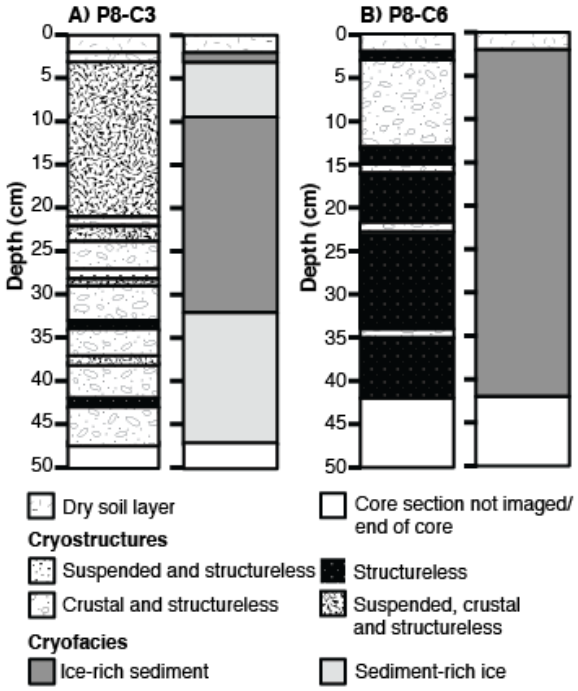

Figure 3: Schematic diagram of cryostructures (derived from CT scan image analysis) and cryofacies (derived from VIC) for A) P8-C3 (center) and B) P8-C6 (left shoulder) cores in University Valley.

The first bulge was shallow (between 5 and 10 cm depth) and narrow, with a maximum value of 57% at ca. 5 cm; the second bulge was broader and reached the highest values (>50%) between ca. 40 and 60 cm depth. The VIC followed a similar trend, but values were higher and ranged from 35 to 69% (not shown). As such, two types of cryofacies were assigned to this core: ice-rich sediment

(>25 to ≤ 50% VIC) and sediment-rich ice (> 50 to ≤ 75% VIC) (Figure 3A).

In core P8-C6, excess ice was present only below 30 cm depth where it ranged between 1 and 3% (Figure 4B). The VIC did not follow the same trend until ca. 30 cm depth, and the VIC values were higher, ranging from 28 to 38% (not shown). Cryofacies within the entire P8-C6 core were defined as ice-rich sediment (Figure 3B).

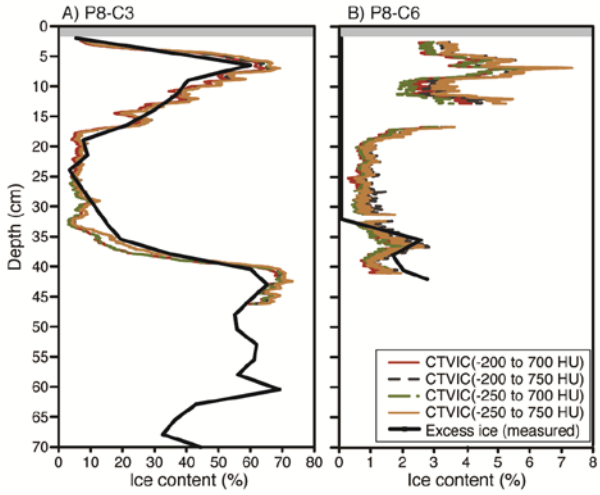

Figure 4: Excess ice content (measured) and volumetric ice contents (derived from CT scan image analysis) for A) P8-C3 (center of polygon) and B) P8-C6 (left shoulder of polygon) cores in University Valley.

4.3 Grain size distribution

Grain size content for core P8-C3 consisted of medium sand, with a predominant grain size of 250 µm (Figure 5A). The distribution of sand-sized particles ranged from 47.3% to 92.1%. Fine-grained sediment (silts and clays) comprised <4.5% of the sediments in the core.

Similarly, the sediment in core P8-C6 (left shoulder of the polygon) was predominantly medium sand, with a dominant grain size of 250 µm (Figure 5B). The distribution of sand-sized particles was slightly higher than in P8-C3, ranging from 66.9% to 96.78%, and the fine-grained sediment comprised <3.5% of the sediments in the core.

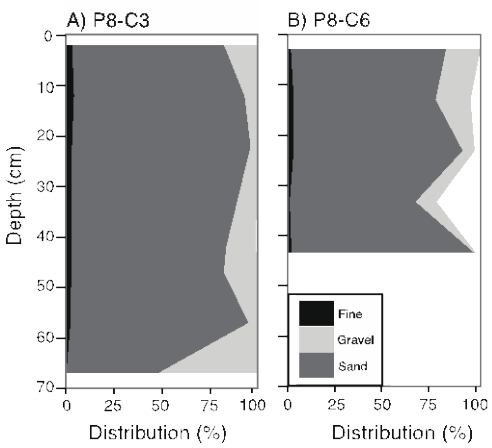

Figure 5: Grain size distribution for A) P8-C3 (center of polygon) and B) P8-C6 (left shoulder of polygon) in University Valley.

5 DISCUSSION

5.1 Digital processing and analysis of permafrost CT-scans to derive ice content

Previous studies have used CT-scanned image analyses of ice-bearing permafrost to extract and quantify VIC values (CT-VIC) (Calmels and Allard, 2004; Calmels and Froese, 2009; Calmels et al., 2010). These studies were performed on ice-rich permafrost samples in peat-rich areas such as the Klondike region in the Yukon and on a palsa in northern Quebec. In the University Valley cores, the CT-VIC and the measured excess ice content were statistically correlated (r^2 = 0.82; p<0.01), but CT-VIC tended to slightly under-estimate excess ice content (Figure 6). On the other hand, CT-VIC was significantly lower than the measured VIC (not shown). The processing and analysis of CT-scanned images can only reveal structures (i.e. ground ice, sediments, gas inclusions) that exceed the image resolution (0.4 mm) (e.g., Calmels and Allard, 2004). With a dominant grain size mode of 250 µm and a porosity of 0.42 ± 0.9 (Lacelle et al., 2013), the pore space in the sediments is slightly less than the pixel resolution of the images and as such, the material within the pore space cannot be spatially resolved. As such, CT-VIC in this type of sediments can be used as a robust first approximation to the presence, abundance and distribution of excess ice only (not pore ice) (Figure 4).

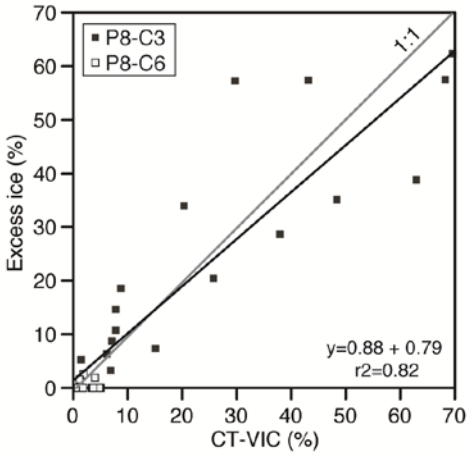

Figure 6: Graph illustrating the CT-VIC values averaged over the same depth interval as the measured excess ice content for P8-C3 and P8-C6.

5.2 Cryostructures in a cold and hyper arid climate

Three types of cryostructures were observed in the shallow ice-bearing permafrost of the investigated polygon: structureless, suspended and crustal. According to studies by Murton and French (1994) and French and Shur (2010), which were based on observations from Arctic permafrost, these types of cryostructures form during the freezing of liquid water. For example, it has been suggested that structureless cryostructures form from the freezing of pore water in sands and gravels; crustal cryostructures, the least common type in Arctic permafrost, form by ice segregation around frost-susceptible clasts; finally, the formation of suspended cryostructures remains elusive as the mechanism(s) by which soil aggregates are suspended during ice segregation or injection is unclear.

The investigated polygon was situated near the fringe of the perennially cryotic zone in University Valley, where air and ground surface temperatures are always <0°C. Further, the δD-δ^{18}O values in both permafrost cores were distributed along a regression slope similar to the local meteoric water line but shifted below it due to low D-excess (Figure 7). This type of distribution has been attributed to vapour deposition (Lacelle et al., 2013; Fisher and Lacelle, 2014). Based on this, we propose that the development of structureless cryostructures in the cores resulted from the diffusion and deposition of water vapour into the pore space of the soil. On the other hand, thermal contraction and expansion of the cryotic soil due to diurnal and annual ground temperature cycles would have generated fractures and cracks that were also filled with ice derived from water vapour, thereby increasing the ice content in the soil above pore-filling space. The combination of ground ice emplacement by vapour-diffusion in the pore space and in larger thermal cracks and fissures could produce suspended and crustal cryostructures. Hence, our results suggest that structureless, suspended and crustal cryostructures can also form from water vapour deposition. Using the REGO model (Fisher, 2005), and based on the climate conditions and soil properties in University Valley, Lacelle et al. (2013) suggested that it would take ca. 225 to 375 years to infill the pore space of the sediments (i.e., to produce the structureless cryostructure) and ca. 12,500 years to reach excess ice content near 80%, assuming stable surface conditions.

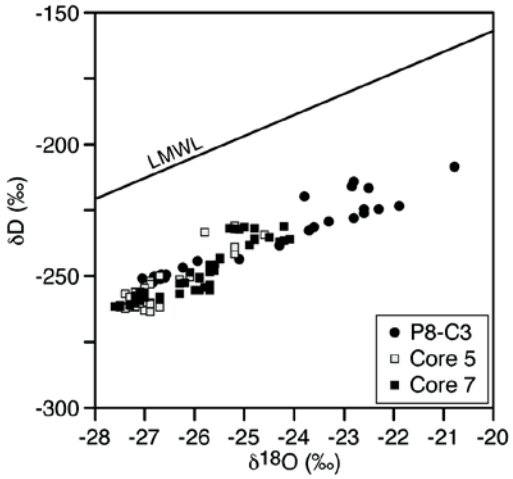

Figure 7: δD-δ^{18}O composition of ground ice in P8-C3 compared to the values from two nearby sites (Core 5 and Core 7; from Lacelle et al., 2013). LWML = local meteoric water line (δD = 7.9 δ^{18}O +0.8; Lacelle et al., 2011).

5.3 Amount and distribution of ground ice in P8

Our results indicate higher VIC and excess ice content in the center of the polygon (P8-C3) than in the shoulder (P8-C6). This illustrates that ice content is spatially variable in an individual polygon over a short horizontal distance (6 x 15 m) and with depth (0 to 70 cm; 0 to 42 cm). This result is similar to the findings of Lacelle et al. (2014) that observed that ground ice contents were highly variable within as little as 5 m. The mechanism responsible for the difference in ice contents between the shoulder and center of the P8 polygon is unclear. McKay (2009) suggested that the presence of a recurring snow cover would increase the humidity above the ground and result in the diffusion and deposition of water into the permafrost below. However, we can assume that if snow is present at the center of the polygon it should, in turn, be present at the shoulder; therefore, a difference in spatial distribution of the snow cover is likely not the factor influencing the variation in ice content. Previous studies from Arctic Canada (e.g. Kokelj and Burn, 2005; O'Neil and Burn, 2012) have documented a relation between ground ice content and grain size of the sediments. However, no relation exists between grain size and ice content in P8-C3 and P8-C6 cores (Figure 8).

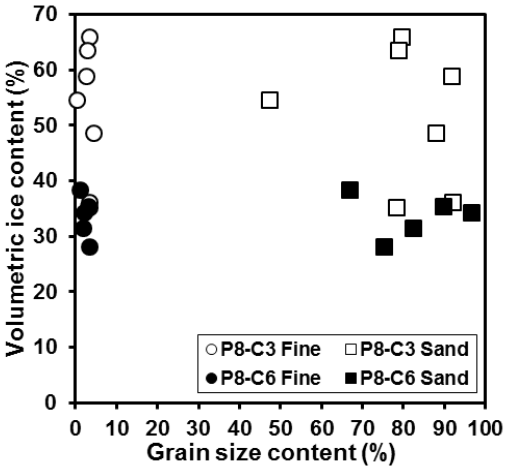

Figure 8: Graph illustrating the comparison of volumetric ice content with grain size distribution for P8-C3 and P8-C6.

Variations in ground ice content could be attributed to the mechanisms responsible for the development of sand-wedge polygons. Cracks in ice-bearing permafrost will form when tensile stresses, resulting from the cooling of the ground surface and subsurface, exceed the tensile strength of the frozen soil (Lachenbruch, 1962). The cracks that open at the surface of the ground are no more than millimeters in width and sand or fine-grained sediments from the dry soil layer may fall into the open crack (Mellon et al., 2013). Therefore, the continued cycle of polygon development causes an unstable surface near the shoulder of the polygon; whereas the center of the polygon experiences much less ground disturbance as tensile stresses are largely relieved near the cracks (e.g. Lachenbruch, 1962). As a result, the sediments near the shoulder are younger than at the center of the polygon. Considering the ground ice in P8 forms by vapour-diffusion and deposition, this would result in a higher ice content in the center of the polygon.

6 CONCLUSIONS

Based on the results from a sand-wedge polygon situated within the perennially cryotic ground, the following conclusions can be reached:

1. CT scanning is a useful tool to investigate cryostructures and ice distribution within medium sand frozen ground in cold and hyper-arid regions.
2. Three different types of cryostructures are found in P8: suspended, structureless and crustal. Volumetric ice content indicates the presence of two types of cyofacies: ice-rich sediment (>25 to ≤ 50% VIC) and sediment-rich ice (> 50 to ≤ 75% VIC). Excess ice is observed across the polygon, ranging from 0 to 57%; however, excess ice content is much greater in the center of the polygon than on the shoulder.
3. The δD-$\delta^{18}O$ composition of ground ice in P8 suggests a vapour-diffusion and deposition origin. Therefore, the presence of structureless, suspended and crustal cryostructures in P8-C3 and P8-C6 suggests vapour diffusion as the process responsible for their formation.
4. The higher ground ice content in the center of the sand-wedge polygon is related to the stability of the ground surface, with a less stable surface near the shoulder of the polygon as sediments fall into cracks.

Future work will investigate the spatial variability (horizontal and vertical) of ground ice within individual polygons along the valley floor, where a switch in ground temperature regime is found (perennially cryotic zone to seasonal non-cryotic zone, where ground surface temperatures may exceed 0ºC for a few hours on clear summer days). Further, the cryostratigraphy of near-surface permafrost in other perennially cryotic zones within the stable upland zone of the MDV should be investigated to assess if the findings in this study can be applied regionally.

ACKNOWLEDGEMENTS

Fieldwork in the MDV was supported by NASA ASTEP program and operated by NSF Office of Polar Programs. NSERC Discovery Grant provided financial support for the laboratory analyses. We would like to thank J. Heldmann, M. Marinova and D. Andersen for field assistance.

REFERENCES

Bockheim, J.G., Campbell, I.B. and McLeod, M. 2007. Permafrost distribution and active layer depths in the McMurdo Dry Valleys, Antarctica, *Permafrost and Periglacial Processes,* 18: 217-227.

Calmels, F. and Allard, M. 2004. Ice segregation and gas distribution in permafrost using tomodensitometric analysis, *Permafrost and Periglacial Processes,* 15: 367-378.

Calmels, F. and Allard, M. 2008. Segregated ice structures in various heaved permafrost landforms through CT scan, *Earth Surface Processes and Landforms,* 33: 209-225.

Calmels, F., Delisle, G. and Allard, M. 2008. Internal structure and the thermal and hydrological regime of a typical lithalsa: significance of permafrost growth and decay, *Canadian Journal of Earth Sciences,* 45: 31-43.

Calmels, F. and Froese, D.G. 2009. Cryostratigraphic record of permafrost degradation and recovery following historic surface disturbances, Klondike area, Yukon. In: Yukon Exploration and Geology 2008, L.H. Weston, L.R. Blackburn and L.L. Lewis (eds.), Yukon Geological Survey, 85-97.

Calmels, F., Clavano, W.R. and Froese, D.G. 2010. Progress on X-ray computed tomography (CT) scanning in permafrost studies, *Geo2010: 63rd Canadian Geotechnical Conference*, Calgary, Alberta, Canada.

Cox, S.C., Turnbull, I.M., Isaac, M.J., Townsend, D.B.,

Smith, B.L. (compilers) 2012. Geology of southern Victoria Land Antarctica. Institute of Geological and Nuclear Sciences, 1:250,000 geological map 22. Lower Hutt, New Zealand, GNS Science. 135pp.

Dickenson, W.W. and Rosen, M.R. 2003. Antarctic permafrost: An analogue for water and diagenetic minerals on Mars, *Geological Society of America,* 31: 199-202.

Elliot, D.H. and Fleming, T.H. 2004. Occurrence and dispersal of magmas in the Jurassic Ferrar large Igneous Province, Antarctica, *Journal of Volcanology and Geothermal Research,* 172: 20-37.

Fisher, D.A. 2005. A process to make massive ice in the martian regolith using long term diffusion and thermal cracking, *Icarus,* 105: 501-511.

Fisher, D. A. and Lacelle, D. 2014. A model for co-isotopic signatures evolving ground ice in the cold dry environments of Earth and Mars, *Icarus,* 243: 454-470.

French, H.M. 1998. An appraisal of cryostratigraphy in North-West Arctic Canada, *Permafrost and Periglacial Processes,* 9: 297-312.

French, H.M. 2007. *The periglacial environment,* 2nd ed., Edinburgh Gate, Harlow, England.

French, H. and Shur, Y. 2010. The principles of cryostratigraphy, *Earth Science Reviews,* 101: 190-206.

Hagedorn, B., Sletton, R.S., Hallet, B., McTigue, D.F. and Steig, E.J. 2010. Ground ice recharge via brine transport in frozen soils of Victoria Valley, Antarctica: Insights from modelling $\delta^{18}O$ and δD profiles, *Geochimica and Cosmochimica Acta,* 74: 435-448.

Hendry, M.J., Barbour, S.L., Zettl, J., Chostner, V. and Wassenaar, L.I. 2011. Controls on the long-term downward transport of δ^2H of water in a regionally extensive, two-layered aquitard system, *Water Resources Research*, 47: W06505.

Kokelj, S.V. and Burn, C.R. 2003. Ground ice and soluble cations in near-surface permafrost, Inuvik, Northwest Territories Canada, *Permafrost and Periglacial Processes,* 14: 275-289.

Kokelj, S.V. and Burn, C.R. 2005. Geochemistry of the active layer and near-surface permafrost, Mackenzie delta region, Northwest Territories, Canada, *Canadian Journal of Earth Sciences*, 42: 37-48.

Lacelle, D., Davila, A., Pollard, W.H., Andersen, F., Heldmann, J., Marinova, M. and McKay, C.P. 2011. Stability of massive ground ice bodies in University Valley, McMurdo Dry Valleys of Antarctica: using stable O-H isotopes as tracers of sublimation in hyper-arid regions, *Earth Planetary Science Letters,* 301: 403-411.

Lacelle, D., Davila, A.F., Fisher, D., Pollard, W.H., DeWitt, R., Heldmann, J., Marinova, M.M. and McKay, C.P. 2013. Excess ground ice of condensation-diffusion origin in University Valley, Dry Valleys of Antarctica: Evidence from isotope geochemistry and numerical modelling, *Geochimica and Cosmochimica Acta,* 120: 280-297.

Lacelle, D., Fontaine, M., Forest, A.P. and Kokelj, S. 2014. High-resolution stable water isotopes as tracers of thaw unconformities in permafrost: a case study from western Arctic Canada, *Chemical Geology,* 368: 85-96.

Lacelle, D., Lapalme, C., Davila, A.F., Pollard, W., Marinova, M., Heldmann, J. and McKay, C.P. 2015. Solar radiation and air and ground temperature relations in the cold and hyper-arid Quartermain Mountains, McMurdo Dry Valleys of Antarctica, *Permafrost and Periglacial Processes,* DOI: 10.1002/ppp.1859.

Lachenbruch, A.H. 1962. Mechanics of thermal contraction cracks and ice-wedge polygons in permafrost, *Geologic Society of America Special Papers,* 70: 1-66.

Mackay, J.R. 1972. The world of underground ice, *ANNALS of the association of American geographers,* 62(1): 1-22.

McKay, C.P. 2009. Snow recurrence sets the depth of dry permafrost at high elevations in the McMurdo Dry Valleys of Antarctica, *Antarctic Science,* 21: 31-38.

Marchant D.R., Phillips, W.M., Moore, E.J., Souchez R.A., Denton, G.H., Sugden, D.E., Potter Jr.,N. and Landis G.P. 2002. Formation of patterned ground and sublimation till over Miocene glacier ice in Beacon Valley, southern Victoria Land, Antarctica, *Geological Society of America,* 144: 718-730.

Marchant, D.R. and Head, J.W.III. 2007. Antarctic dry valleys: Microclimate zonation, variable geomorphic processes, and implications for assessing climate change on Mars, *Icarus,* 192: 187-222.

Marinova, M.M., McKay, C.P., Pollard, W.H., Heldmann, J.L., Davila, A.F., Anderson, D.T., Jackson, W.A., Lacelle, D., Paulsen, G. and Zacny, K. 2013. Distribution of depth to ice-cemented soils in the high elevation Quartermain Mountains, McMurdo Dry Valleys, Antarctica, *Antarctic Science,* 25: 575-582.

Mellon, M.T., McKay, C.P. and Heldmann, J.L. 2013. Polygonal ground in the McMurdo Dry Valleys of Antarctica and its relationship to ice-table depth and the recent Antarctic climate history, *Antarctic Science*, 26: 413-426.

Murton, J.C. and French, H.M. 1994. Cryostructures in permafrost, Tuktoyaktuk coastlands, western arctic Canada, *Canadian Journal of Earth Sciences,* 31: 737-747.

O'Neil, H.B. and Burn, C.R. 2012. Physical and temporal factors controlling the development of near-surface ground ice at Illisarvik, western Arctic coast, Canada, *Canadian Journal of Earth Sciences*, 49: 1096-1110.

Pollard, W.H., Lacelle, D., Davila, A.F., Andersen, D., McKay, C.P., Marinova, M. and Heldman, J. 2012. Ground ice conditions in University Valley, McMurdo Dry Valleys, Antarctica, *Tenth International Conference on Permafrost*, Salekhard, Yamal-Nenets, Autonomous District, Russia: 305-310.

van Everdingen, R. (Ed.). *Multi-language glossary of permafrost and related ground-ice terms*, Boulder, CO, USA.